Journal of Photochemistry and Photobiology A: Chemistry 203 (2009) 192–198

Contents lists available at ScienceDirect

Journal of Photochemistry and Photobiology A: Chemistry

journal homepage: www.elsevier.com/locate/jphotochem

Sol–gel modified TiO_2 powder films for high performance dye-sensitized solar cells

Yongjun Chen [a], Elias Stathatos [b,*], Dionysios D. Dionysiou [a,**]

[a] Department of Civil and Environmental Engineering, University of Cincinnati, Cincinnati, OH, 45221- 0071, USA
[b] Department of Electrical Engineering, Technological-Educational Institute of Patras, M. Alexandrou 1, GR-263 34 Patras, Greece

ARTICLE INFO

Article history:
Received 23 September 2008
Received in revised form 8 December 2008
Accepted 31 January 2009
Available online 10 February 2009

Keywords:
Dye-sensitized solar cells
Degussa P25
Ishihara ST-01
Quasi-solid state electrolyte
TiO_2 thick films
Sol–gel

ABSTRACT

Techniques in TiO_2 film fabrication process are a very important aspect in construction of efficient dye-sensitized solar cells (DSSCs). Among fundamental factors in high efficiency solar cells is the development of a highly porous nanocrystalline film in a relatively thick and mechanical stable TiO_2 network. In present work, two types of commercial titania powders with high loading (74% (wt.%) in the final films), Degussa P25 powders and Ishihara ST-01 powders, have been successfully incorporated into a mesoporous structured TiO_2 crystalline network. The good mechanical stability of both types of films involves the presence of a titanium alkoxide solution mixed with non-ionic surfactant Tween 20 as a suitable binder precursor to immobilize commercial titania nanoparticles on a SnO_2:F conductive glass via a dip coating sol–gel process. The results of photoelectrochemical characterization of the films in a dye-sensitized solar cell showed that both films presented high conversion efficiency (about 6%) with only a slight difference on their photovoltaic behavior, when a quasi-solid state electrolyte was employed. The crystalline structure of the foreign titania particles, the particle size and the existence of any agglomeration, as well as the surface area and the pore structure of these films made of different titania powder sources were examined in detail and are discussed in relation to the relatively high solar to electrical energy conversion efficiency obtained in such quasi-solid state DSSCs.

1. Introduction

Since the first report on an overall efficiency of 7.1–7.9% of dye-sensitized TiO_2 solar cells by O'Regan and Grätzel in 1991, nanocrystalline TiO_2, a wide band gap semiconductor material (i.e., anatase 3.2 eV), has been extensively investigated as an effective electrode material for the application in dye-sensitized solar cells (DSSCs) [1–12]. In order to obtain a high photovoltaic performance of the TiO_2 solar cells, generally, the TiO_2 electrode material should have (i) a relatively large film thickness (~10 μm) and high BET surface area to adsorb enough amount of dye for good solar light harvesting, and (ii) interconnected crystalline network for effective electron transfer from dye molecules [11–14]. Therefore, the design and development of TiO_2 films with such structure becomes an important topic in the field of dye-sensitized solar cells. Recently, employing commercial TiO_2 nanoparticles (i.e., Degussa P25) as building blocks to fabricate thick TiO_2 films has attracted great attention [11,15,16], because of their high purity, availability, and relatively low cost. Furthermore, incorporating TiO_2 nanoparticles as nanofillers into titanium alkoxide solution to form composite film has been proved to be a promising technique to prepare thick TiO_2 coatings for water and air purification [17–21] as well as dye-sensitized solar cells [11,12]. Moreover, incorporating catalytically active nanoparticles into mesoporous materials is also a promising strategy to synthesize new catalytic materials [22]. The relationship of foreign TiO_2 particles with TiO_2 formed from titanium sol precursor via hydrolysis/condensation and crystallization process was in fact "host"–"guest" relationship in the composite films. When the composition of foreign TiO_2 particles was dominant in the composite films (i.e., above 50%, (wt.%)), the TiO_2 films formed from titanium sol (no foreign TiO_2), essentially functioned as a catalytic active binder (matrix) to immobilize foreign TiO_2 particles on the substrate [23]. The advantage of using this technique for the preparation of TiO_2 films is that the high purity commercial TiO_2 nanoparticles can be well "glued" by the presence of sol–gel derived TiO_2 matrix. As a result, good electron transport properties of the as-prepared films via a high temperature calcination procedure can be obtained.

In this study, we employed two types of commercial titania particles, Degussa P25 and Ishihara ST-01, and incorporated them into a mesoporous TiO_2 matrix prepared from a Tween 20 surfactant associated titanium alkoxide precursor sol. SnO_2:F transparent

* Corresponding author. Tel.: +30 2610 369242; fax: +30 2610 369299.
** Co-corresponding author. Tel.: +1 513 556 0724; fax: +1 513 556 2599.
E-mail addresses: estathatos@teipat.gr (E. Stathatos), dionysios.d.dionysiou@uc.edu (D.D. Dionysiou).

1010-6030/$ – see front matter © 2009 Elsevier B.V. All rights reserved.
doi:10.1016/j.jphotochem.2009.01.019

conductive glass (FTO) was employed as the support because high temperature calcination has less effect on its resistance compared with Sn-doped In_2O_3 (ITO) [24]. Titania powder modified films were produced using a dip coating sol–gel process, a simple and important technique to coat TiO_2 film on a support with various shapes and dimensions [25]. Finally, film structure and photovoltaic behavior are compared to each other. The purpose of this study was to obtain insights of the relationship of film structure to the photovoltaic behavior of these types of films. This can help to provide a basis on the microstructure design of commercial TiO_2 nanoparticle based composite coatings for effective solar light harvesting and fast interfacial charge transfer, which are two important factors affecting the efficiency of dye-sensitized solar cells.

2. Experimental

2.1. Materials

Potassium iodide, iodine, 1-methyl-3-propylimidazolium iodide, hydrogen hexachloroplatinate(IV) hydrate (H_2PtCl_6), poly (propylene glycol)bis(2-aminopropyl) ether, 3-isocyanatopropyltriethoxysilane and all solvents were purchased from Sigma–Aldrich. Cis-bis(isothiocyanato)bis(2,2′-bipyridyl-4,4′-dicarboxylato)-ruthenium(II) ($RuL_2(NCS)_2$—N3) was provided by Solaronix SA (rue de l'Ouriette 129, 1170 Aubonne VD, Switzerland). SnO_2:F transparent conductive electrodes (FTO, TEC15) 15 Ω/sq were purchased from Hartford Glass Co., USA. Commercial ultra pure titanium isopropoxide (TTIP, 97%, Aldrich), 1-butanol (anhydrous, 99.8%, Aldrich), and acetylacetone (99%, Fisher Scientific) was used to make precursor Ti sol. Highly sticky non-ionic surfactant Tween 20 (Aldrich) is used to improve the sol viscosity and function as the structure-directing agent. Degussa P25 powders were provided by Degussa Company (30% rutile and 70% anatase, mean particle diameter of 30 nm, BET surface area of about 50 m^2/g). ST-01 was also a commercial TiO_2 product (above 99.9% purity, anatase, mean particle diameter of 7 nm, BET surface area of about 300 m^2/g, Ishihara).

2.2. Preparation of TiO_2 films

First, an alcoholic solution was prepared, which included acetylacetone (0.26 M), TTIP (0.45 M), H_2O (0.91 M) and 1-butanol as a solvent. Then, Tween 20 was added under vigorous stirring in 1:1 volume ratio with 1-butanol sol. As a result, the molar ratio of Tween 20:TTIP:H_2O:acetylacetone:1-butanol is 1:4.7:9.5:2.7:93.3. The Tween 20 associated Ti sol is transparent and shows a shallow orange color. For the synthesis of titania powder modified films, Degussa P25 nanoparticles or Ishihara ST-01 nanoparticles with 50 g/L loading in the sol were directly added in Tween 20 associated 1-butanol sol under vigorous stirring. Before dip coating of the conductive glass, the P25 powder modified sol or ST-01 powder modified sol was treated in an ultrasonic apparatus for about 3 min to avoid the formation of larger titania agglomerates in the sol.

The dip coating apparatus and high temperature furnace are the same as those reported in former publications [19–21]. A constant withdrawal velocity of 12.3 ± 0.5 cm min^{-1} was employed in the dip coating process. After each FTO conductive glass was dipped into the sol and taken out, the coated gel with ~1 cm^2 (1 cm × 1 cm) area was obtained by removing the adhesive tape used as a mask cut. The furnace temperature was incremented at a ramp rate of 15 °C min^{-1} to 500 °C; this temperature was held for 15 min, then the coated FTO conductive glass was cooled to room temperature. As a result, two types of films, P25 powder modified film (PPMF) and ST-01 powder modified film (STPMF), were synthesized. The result of energy dispersive X-ray spectrometer (EDS) analysis proved that no measurable carbon composition in the as-prepared films can be detected, which suggested that organic contents could be eliminated after calcination at 500 °C and depending also on the time of the heat treatment.

2.3. Film characterization

The crystal phase composition of both types of titania powder modified films and their TiO_2 matrix (without P25 or ST-01) were determined by X-ray diffraction (XRD) using a Siemens Kristalloflex D500 diffractometer with CuKa radiation. Film morphology and film thickness were characterized by Scanning Electron Microscopy (SEM; Hitachi S-4000). Residual organic composition of the films was examined by energy dispersive X-ray spectroscope (EDX, Oxford Isis) with windowless EDS detector. BET surface area and pore structure were analyzed by Micromeritics TriStar 3000 Gas Adsorption Analyzer. Powder samples were obtained by scratching titania powder modified films (3 dip coating layers) from the FTO conductive glass. For TiO_2 matrix (without P25 or ST-01), powder samples obtained from TiO_2 "films" (1 layer) coated on FTO glass prepared at the same operation conditions were also characterized for comparison. All particle samples were degassed at 180 °C for 150 min before N_2 adsorption and desorption analysis. High Resolution-Transmission Electron Microscope (HR-TEM) with field emission gun at 200 kV was employed to examine crystal network structure. Before TEM analysis was performed, the powder samples dispersed in methanol (HPLC grade, Pharmco) were treated using an ultrasonic cleaner (2510R-DH, Bransonic) for 5 min and fixed on a carbon-coated copper grid (LC200-Cu, EMS). UV–vis spectra of the titania powder modified films and the TiO_2 matrix were obtained using a UV-vis spectrophotometer (Hewlett Packard 8452A). The apparent viscosities of the titania powder modified sols were measured by a Brookfield rotational viscometer (DV-E) with ultra-low adapter (3.0 rpm).

2.4. Preparation of quasi-solid state electrolyte for dye-sensitized solar cells

In the construction of the solar cells a quasi-solid state electrolyte was used. This was chosen as a promising approach to DSSC technology as it combines the high ionic conductivity of liquids while it reduces the risk of leaks and minimizes sealing problems in the cells. For the gel electrolyte applied to the DSSCs, we used a hybrid organic–inorganic material ICS-PPG230 which was prepared according to a procedure described in a previous publication [16]. Briefly, poly(propylene glycol)bis(2-aminopropyl ether) of molecular weight 230 and 3-isocyanatopropyltriethoxysilane (ICS; molar ratio ICS/diamine = 2) react in a vessel (acylation reaction), producing urea connecting groups between the polymer units and the inorganic part. The gel electrolyte was synthesized by the following procedure. 0.7 g of the functionalized alkoxide precursor ICS-PPG230 were dissolved in 2.4 g of sulfolane under vigorous stirring. Then, 0.6 ml glacial acetic acid (AcOH) were added followed by 0.3 M 1-methyl-3-propylimidazolium iodide, 0.1 M KI and 0.05 M I_2 in a final molar ratio AcOH:KI:MPImI:I_2 = 2.5:0.1:0.3:0.05. 1-Methyl-3-propylimidazolium iodide was used in order to avoid crystallization of KI, while the presence of KI was necessary since these small mobile ions allow increase of ionic conductivity. After 6 h stirring, one drop of the obtained sol was placed on the top of the titania electrode with adsorbed N3 dye molecules (from 10^{-3} M ethanolic solution) and a slightly platinized SnO_2:F counter electrode was pushed by hand on the top. The platinized FTO glass was made by exposing it to a H_2PtCl_4 solution (5 mg/1 ml of EtOH) followed by heating at 450 °C for 10 min. The two electrodes tightly stuck together by Si–O–Si bonds developed by the presence of ICS-PPG230.

2.5. Photophysical and electrical characterization of the DSSCs

For the *J–V* characteristic curves, the samples were illuminated with a Newport 300W Xenon lamp. The Xe lamp spectrum satisfactorily simulates solar radiation at the surface of the earth. A water filter with fused silica windows was used to cut infrared irradiation. Newport Air Mass (AM 0 and AM 1.5 direct) filters were used in combination to simulate AM 1.5 direct solar irradiance. The spectral output of Xe lamp was matched in the region of 350–800 nm with the presence of Prinz IR3 heat-reflecting sunlight filter (Prinz Optics, GmbH) so as to reduce the mismatch between the simulated and the true solar spectrum to less than 3%. The number of incident photons was calculated by employing a radiant power/energy meter (Oriel-70260). Photodiode detector was individually calibrated against NIST traceable standards. In addition, the calibration was corrected for different wavelengths. The accuracy in measurement was generally ±3%. Finally, the *J–V* curves were recorded by connecting the cells to a Keithley Source Meter (model 2601) which was controlled by Keithley computer software (LabTracer). Cell active area for these measurements was finally 0.95 cm^2. Not any masks and back reflectors were used in all measurements. Cell performance parameters, including short circuit current density (J_{SC}), open circuit voltage (V_{OC}), maximum power (P_{max}), fill factor (*ff*) and overall cell conversion efficiency, were measured and calculated from each *J–V* characteristic curve. Finally for each case of TiO_2 films, we have made three cells which were tested under the same conditions in order to avoid any misleading estimation of their efficiency.

3. Results and discussion

3.1. Optical properties of the films

In order to confirm that 3 dip coating layers of the two types of films have enough film thickness for the light adsorption by dye molecules, the optical properties of the films were firstly investigated. Fig. 1 shows the transmittance spectra of PPMF and STPMF films, the TiO_2 matrix and bare FTO conductive glass after 500 °C calcination (3 times heating treatment cycles, total 45 min). Before making sample analysis, a bare FTO conductive glass was used as a blank. It was found that 500 °C calcination could not affect the transmittance of bare FTO conductive glass. Therefore, the transmittance spectra of P25–TiO_2 composite film and its TiO_2 matrix represent the film properties. Both titania powder modified films (3 layers) are opaque without light penetration at the wavelength range of 320–800 nm. Therefore, 3 dip coating layers of the titania powder modified films are enough to absorb UV–vis light. On the other hand, it was observed that the TiO_2 matrix exhibited high transmittance (i.e., above 80%, 6 layers) at the wavelength range from 400 nm to 800 nm. Therefore, the titania powder modified films coated on FTO conductive glass is, essentially, the immobilization of high loading commercial titania nanoparticles using a TiO_2 matrix with large light transmittance at the visible light range (i.e., above 400 nm). Such a transparent TiO_2 matrix is believed to have less effect on the light harvesting of dye molecules adsorbed on Degussa P25 or ST-01 nanoparticles in the visible light range. Considering the fact that electrolyte solution and dye molecules cannot lead to an improvement in UV light penetration in the film, the conclusion about optical properties of the layers is, that the transmittance of PPMF and STPMF is 0%, suggesting that the films attached by dye molecules have 100% light absorption in the cells.

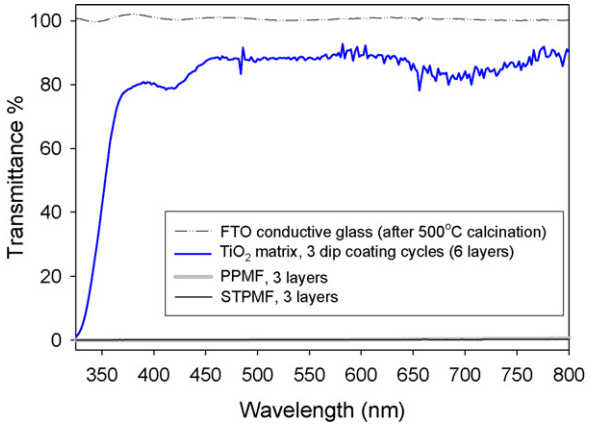

Fig. 1. Transmittance of two types of TiO_2 films and their TiO_2 matrix.

3.2. Crystalline structure and crystalline network

Fig. 2(i) shows the results of XRD spectra of the two types of composite films coated on FTO conductive glass and bare FTO conductive glass Fig. 2(i, a). Distinctive peaks at 2θ angle of 25.4° and 27.5° can be observed in Fig. 2(i, b), which suggests that there is large amount of Degussa P25 crystalline composition in the PPMF. In fact, the amount of Degussa P25 composition or ST-01 composition in the each film reaches 74% (wt.%), a high commercial TiO_2 loading in the film. On the other hand, an obvious peak at 2θ angle of 25.4° can be observed in Fig. 2(i, c), which suggests there is only anatase TiO_2 crystalline composition in the STPMF. The peak intensity of PPMF is higher than that of STPMF, which suggests that PPMF has a larger amount of titania. In Fig. 2(i, a), the peaks corresponding to SnO_2 crystalline composition can be observed. This is due to the existence of SnO_2 crystalline layer on the FTO conductive glass. Compared with the full width at half-maximum intensity

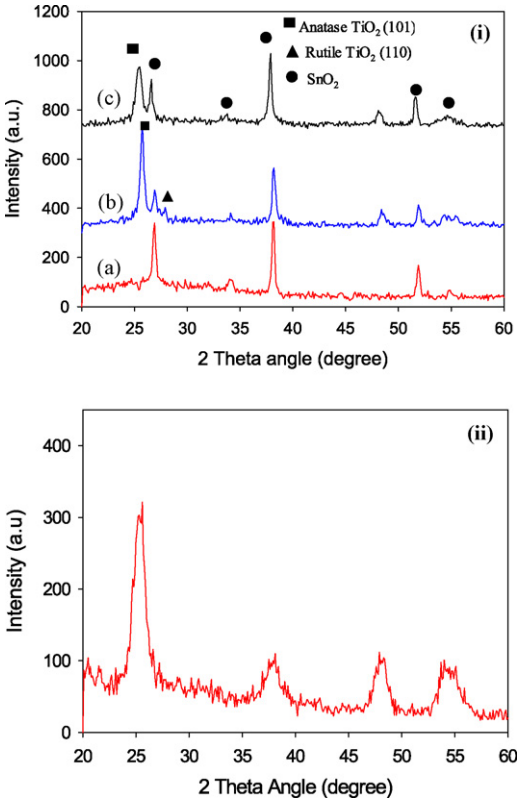

Fig. 2. (i) XRD spectra of titania powder modified films (a) FTO glass as reference, (b) PPMF and (c) STPMF. (ii) TiO_2 matrix formed from titanium sol solution (without P25 or ST-01).

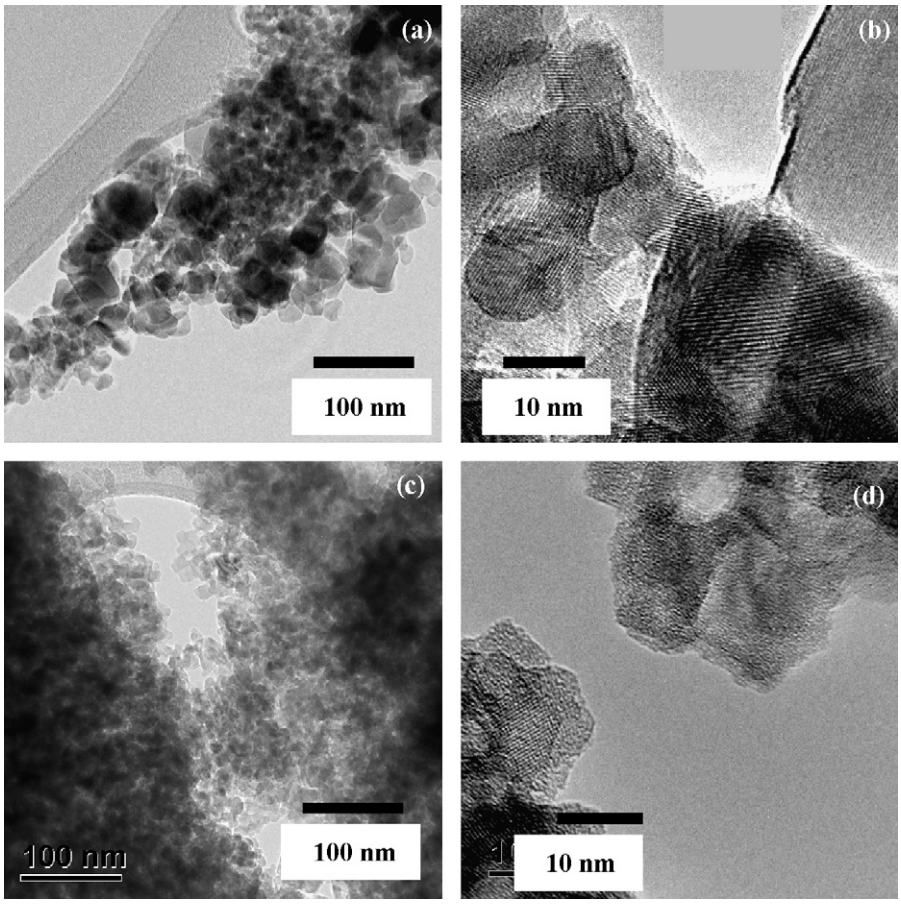

Fig. 3. HRTEM images of titania powder modified films. Adding Degussa P25 (a) and (b), adding ST-01 (c) and (d). (Sample scratched from 3 dip coating layers, 500 °C, (a) and (c) low magnification, (b) and (d) high magnification.)

(FWHM) of anatase (1 0 1 plane) in the PPMF and in the STPMF, larger FWHM of STPMF suggests a smaller average crystalline size, which can be easily explained to be due to the small crystalline size of ST-01 nanoparticles. In order to obtain information on the crystalline structure of TiO_2 matrix, which is formed via a surfactant self-assembling sol–gel process after 500 °C calcination, the powder sample scratched from TiO_2 film (without Degussa P25 or ST-01) on FTO conductive glass was also analyzed using XRD. From Fig. 2(ii), it can be concluded that the TiO_2 matrix has been well crystallized into anatase crystalline phase. Considering the fact that interconnected crystalline network is an important structural property to obtain an effective electron transfer from the dye molecules in dye-sensitized solar cells [11], the crystalline network of the film was also observed by HRTEM analysis. The results are shown in Fig. 3. From Fig. 3(a) and (b), it can be observed that PPMF has interconnected crystal network with small size of crystallites (8–10 nm) as pore wall of small inter-particle pores (i.e., 3–5 nm). PPMF has also large pores (i.e., ~35 nm) with larger particles (i.e., about 30 nm, Degussa P25) as pore walls. On the other hand, compared with that of PPMF, STPMF has smaller and "uniform" crystalline size (8–10 nm) and smaller inter-particle pores (refer to Fig. 3(c) and (d)). The overall TEM images of the two types of films in Fig. 3 suggest that all nanocrystallites, small particles and larger particles, are well-connected to each other although the powder samples have been treated using an ultrasonic apparatus. Based on TEM images in Fig. 3 (b) and (d), the crystalline lattices on the particles also suggest a good crystallization of the two types of films. Therefore, it can be concluded that both types of titania powder modified films possess well-interconnected and porous crystalline network. It has been reported that the presence of larger nanoparticles are beneficial to the enhancement of light reflection, which can lead to enhancement in red light harvesting [11,26], while smaller nanoparticles can provide large BET surface area for the adsorption of large amount of dye molecules [26]. Although it is possible that electron transporting of injected electrons from dye can become less effective for mixed phase Degussa P25 titania, unique crystalline structure with the mixture of large and small particles in PPMF was anticipated to have high solar energy conversion efficiency.

3.3. Textural properties of the films

The texture of the two types of titania powder modified films and the TiO_2 matrix were analyzed by N_2 adsorption and desorption. The results are shown in Fig. 4(a)–(c). In addition, their BET surface area and pore structure are also summarized in Table 1. From Fig. 4, it can be observed that incorporating commercial titania powders into the sol can lead to a remarkable change on the textual structure of the final films. After Degussa P25 particles are incorporated into TiO_2 matrix, the hysteresis loop shifts from a lower relative pressure region ($0.4 < P/P_0 < 0.8$) to a higher relative pressure region ($0.8 < P/P_0 < 1.0$), which suggests that Degussa P25 particles could lead to the formation of larger pores [20,21]. For STPMF, incorporating ST-01 nanoparticles into TiO_2 matrix leads to formation of enhanced mesopore structure. Moreover, STPMF has relatively narrow pore size distribution with average pore size of 18.8 nm. Therefore, the inter-agglomerate pores (i.e., 18.8 nm) are dominant in the total pore volume of the STPMF. On the other hand, PPMF has a wide pore size distribution with the formation of larger mesopores (i.e., ~35 nm). Such large pores are expected to have a

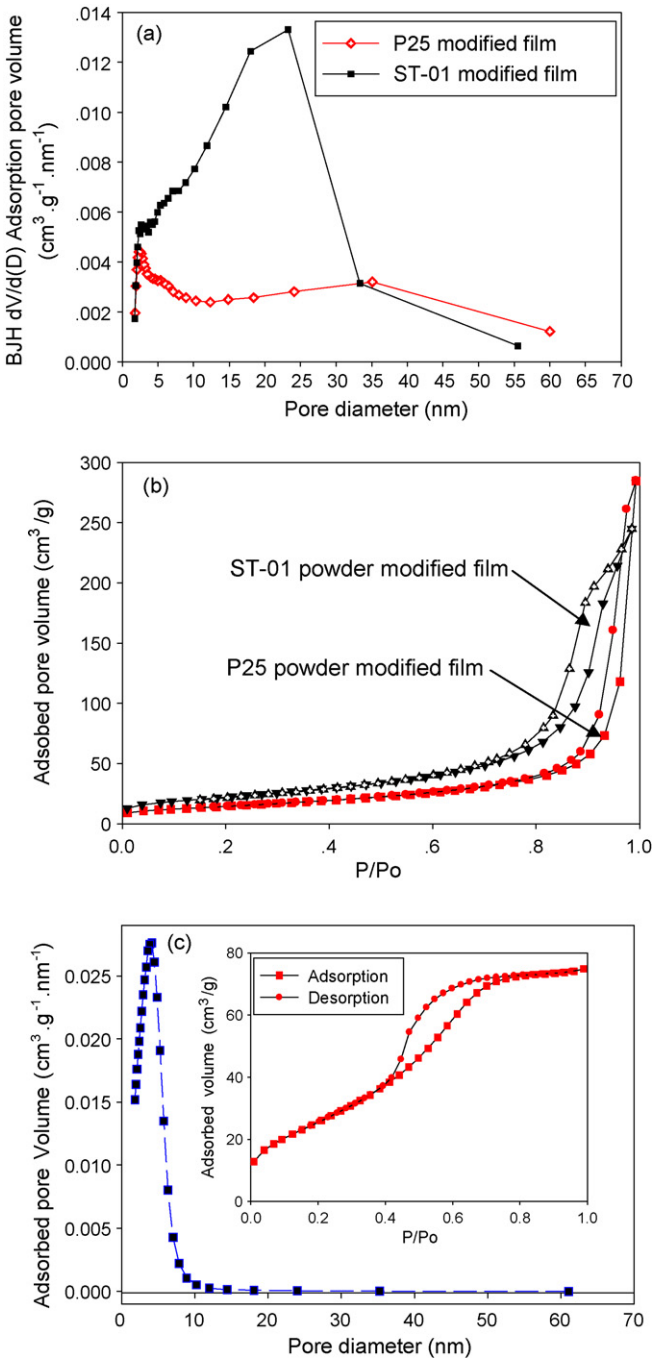

Fig. 4. (a) Pore size distribution of titania powder modified films, (b) adsorption and desorption isotherms of titania powder modified films, and (c) adsorption and desorption isotherm and pore size distribution of TiO_2 matrix.

beneficial effect on the electrolyte solution wetting and filling in the TiO_2 films [14] and good light harvesting [27].

3.4. Surface morphology, film thickness and hydrophilicity

As shown in Fig. 5(a) and (b), both films exhibit rough surface morphology with small crack formation which are few more in the case of STPMF. Because increasing the number of foreign titania particles leads to an enhancement in the air–liquid contact area of the coated sol attached on foreign titania particles, drying rate of the sol increases. Therefore, higher stress induced by higher drying rate of the sol for the STPMF is believed to be an important reason to produce larger number of cracks. Although crack formation has a detrimental effect on the mechanical stability of the film, no obvious peeling off for the titania powder modified films was observed after they had been dipped into dye solution. Therefore, these films still have good "mechanical stability" for the application of dye-sensitized solar cells. It is believed that consolidated crystal network and strong chemical bonds (i.e., Ti–O–Sn) between the titania film and FTO conductive glass induced by high calcination temperature (i.e., 500 °C) are two important factors contributing to such a good mechanical stability. Considering the fact that film thickness is an important factor to affect photovoltaic behavior of the cells, the film thickness of two types of films was also investigated using cross-section SEM technique. A comparable film thickness of the two types of films can be observed (refer to Fig. 6 and Table 1), while STPMF presented a rougher surface than PPMF. As an example, Fig. 6(a) and (b) shows the result of cross-section SEM analysis on parts of the films. Fig. 6(a) clearly shows a rough surface of STPMF, which is induced by the existence of larger agglomerates in the film. Larger agglomerate in the sol can lead to the formation of higher numbers of "large mountains" or "large islands" in the film, which is an important factor leading to the large film thickness of STPMF. On the other hand, some larger inter-agglomerate pores with dimensions above 300 nm can be occasionally observed in STPMF. Such larger inter-agglomerate pores cannot lead to a capillary condensation during N_2 adsorption and desorption analysis. As a result, they do not have contribution to the pore volume/pore size of STPMF, which is measured by Tristar 3000 instrument. Therefore, the existence of larger inter-agglomerate pores (above 300 nm) as well as some "ditches" in STPMF leads to smaller film weight of STPMF in comparison with that of PPMF, which has been confirmed in our experiments.

Furthermore, we examined the hydrophilicity of both TiO_2 films in order to have an approximation of the number of hydroxyl groups on titania surface and also provide an assessment to the dye access in the pores of the films. Our results showed that both films possess super-hydrophilicity (i.e., contact angle less than 3°) and as a consequence a high content of hydroxyl groups are present on titania surface which are absolutely necessary for the successful adsorption of N3 dye to the TiO_2 surface. This can be explained by the rough surface of the films with combined effect of various pore channels and cracks or "small ditches", which may provide enough capillary

Table 1
Crystallinity, BET surface area, pore volume, and pore size of the films.

TiO_2 film	Crystallinity	BET surface area (m^2/g)	Pore volume (cm^3/g)[a]	Porosity (%)[b]	Pore size (nm)[c]	Film thickness (μm)
TiO_2 matrix[d]	Anatase	101.4	0.1158	31.11	4.6	–
ST-01–TiO_2 particles[e]	Anatase	80.5	0.3787	59.62	18.8	4.5–5.5
P25–TiO_2 particles[e]	Anatase and rutile	52.7	0.3696	59.41	28.1	4.5–5.0

[a] Single point adsorption total pore volume of pores.
[b] Based on pore volume and 3.9 g/m^3 of anatase density. Porosity (%) = pore volume (cm^3/g)/(pore volume (cm^3/g) + solid catalyst volume without pore (cm^3/g)) × 100; solid catalyst volume without pore (cm^3/g) = 1/density of the solid catalyst volume without pore.
[c] Adsorption average pore width (4 V/A by BET).
[d] Sample was scratched from TiO_2 film without foreign titania powder added (1 layer) on FTO conductive glass.
[e] Powder sample was obtained by scraping the film (3 dip coating layers) out of FTO conductive glass.

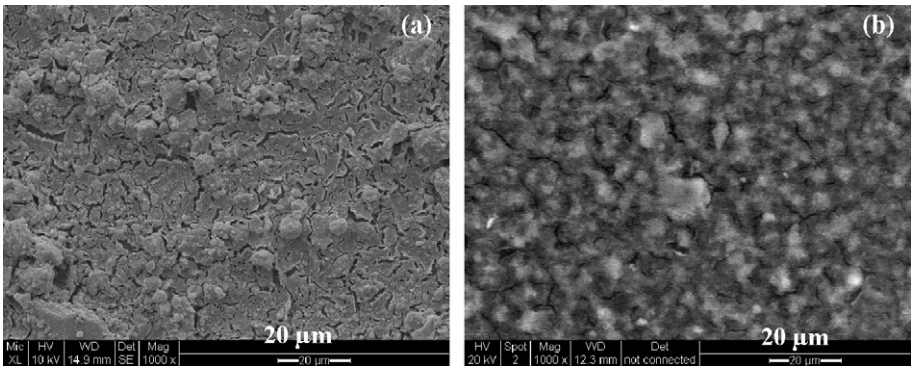

Fig. 5. Scanning electron micrographs of the titania powder modified films. (a) Adding ST-01 and (b) adding Degussa P25.

force to suck water into the film. Therefore, the as-prepared films are also suitable for the development of dye-sensitized solar cells. Usually, ethanol is a common solvent used for N3 dye dilution and then adsorption on TiO_2 films during DSSC construction. Considering the fact that the surface tension of ethanol solvent is only one-third that of water, such a high capillary force is believed to be important for the attachment of dye molecules dissolved in the ethanol solvent at the surface of TiO_2 nanocrystallites in the inner layers of the films.

3.5. Characterization of the dye-photoelectrochemical solar cell performance

The current–voltage (*J–V*) characteristic curves of quasi-solid state dye-sensitized solar cells for both TiO_2 films are presented in Fig. 7. For each case of TiO_2 films, we made three cells which were tested under the same conditions and the data presented below concern the average values obtained from the cells. As it can be seen, the quasi-solid state DSSCs constructed with TiO_2 films employing different titania powders showed almost the same energy to power efficiencies under AM 1.5 simulated Xe-light of 100 mW/cm^2 but finally in the case of P25 modified TiO_2 film (PPMF) the overall

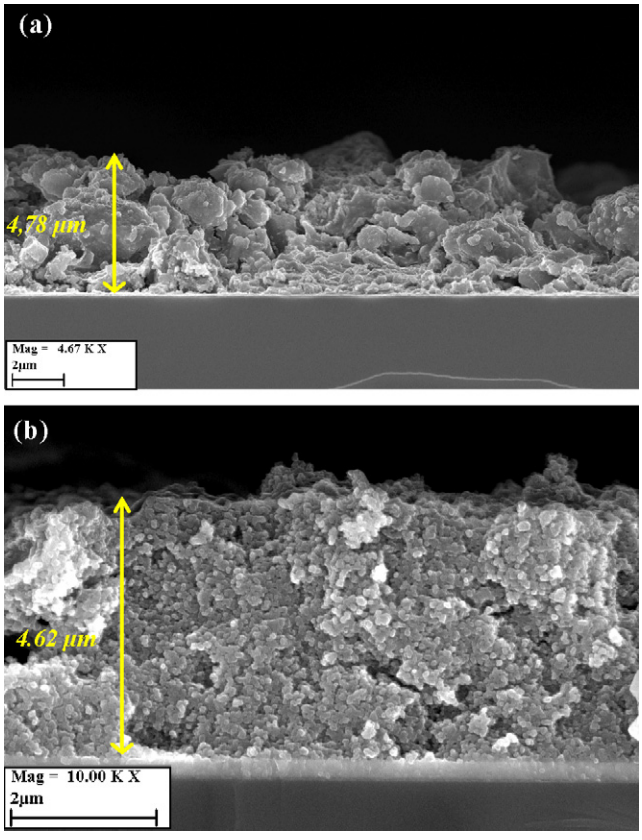

Fig. 6. Cross-sectional FE-SEM images of (a) ST-01 and (b) Degussa P25 powder modified films.

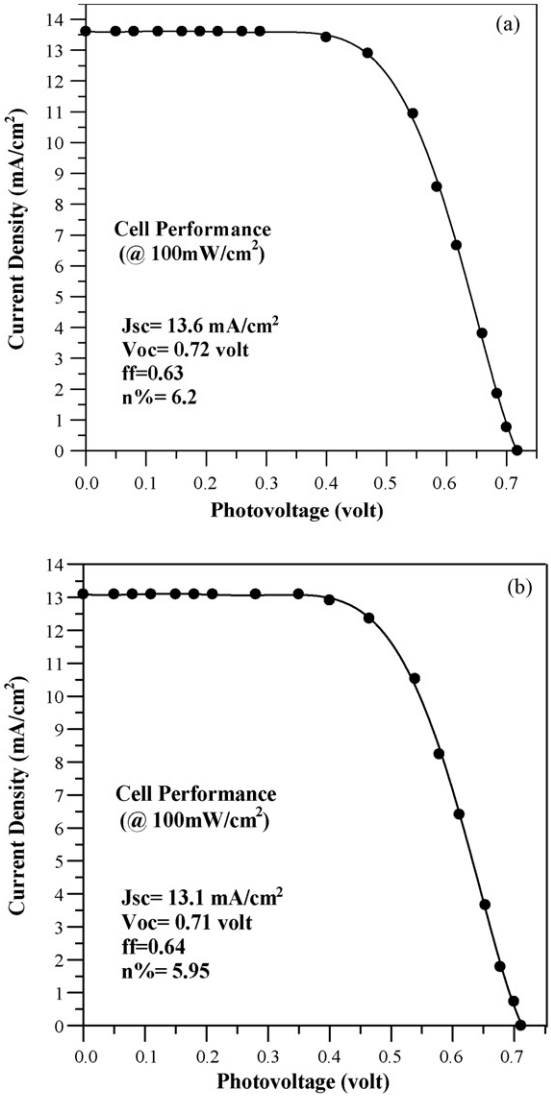

Fig. 7. *J–V* curves at simulated AM 1.5 1 sun Xe-light for the DSSCs constructed with (a) PPMF and (b) STPMF titania powder.

efficiency was slightly higher than the case of ST-01 powder modified TiO_2 film (STPMF). In particular, the open circuit voltage for PPMF sample was 0.72 V and the short circuit current was 13.6 mA/cm^2. The overall efficiency for this cell was measured to be 6.2%. For the second cell STPMF, with exactly the same electrolyte composition, the open circuit voltage was measured 0.71 V and the short circuit current was 13.1 mA/cm^2. The overall efficiency for this cell was slightly decreased to 5.95%. In both cases, the active area of all cells was 0.95 cm^2. We attribute the slight difference in overall efficiencies of the cells to the different textural and morphological characteristics of the two kinds of films as they were described in Sections 3.2 and 3.3 but with the acceptance that there was not any exclusive contribution of any of the characteristics that were described therein. Furthermore the presence of the quasi-solid state electrolyte seems to perfectly collaborate with titania substrate in both cases by giving a high energy to power conversion efficiency, among the best ever recorded for quasi-solid state electrolytes [28–30].

Internationally accepted ageing tests have not yet been established for organic-based solar cells considering the stage of development of these cells [31]. Both devices showed good stability when subjected to 1 sun light irradiance from the Xe lamp as solar simulated light source. After 1000 h of light soaking (6 weeks) under open circuit conditions there was ~10% drop to the overall efficiency at both cells. The cells were all unsealed and also were used without any further treatment after the electrolyte was gelled.

4. Conclusions

This study presents a new method for the preparation of TiO_2 nanocrystalline films for the fabrication of TiO_2 electrodes in dye-sensitized solar cells. A highly transparent and mesoporous TiO_2 matrix can immobilize fine commercial TiO_2 nanoparticles (Degussa P25 and Ishihara ST-01) with high loading on the FTO conductive glass via a dip coating sol–gel process. A quasi-solid electrolyte was used for the fabrication of DSSCs. The constructed solar cells showed high solar to electrical energy conversion efficiency (~6%) and also good long-term stability under 1 sun and 1.5 AM light irradiance. The type of commercial TiO_2 nanoparticles (P25 and ST-01) did not have an obvious effect on the open circuit voltage, the short circuit current, and the overall solar energy conversion efficiency obtained on these films. One of the important findings in this study is a high photovoltaic behavior of the cell could be obtained by only optimizing some structural properties without considering the types of commercial titania particles.

Acknowledgements

Prof. D.D. Dionysiou acknowledges financial support from the Center of Sustainable Urban Engineering (SUE) at the University of Cincinnati and also partial funding from the National Science Foundation through a CAREER award (BES, # 0448117).

References

[1] B. O'Regan, M. Grätzel, Nature (Lond.) 353 (1991) 737.
[2] M. Zukalová, J. Procházka, A. Zukal, J.H. Yum, L. Kavan, Inorg. Chim. Acta 361 (2008) 656.
[3] M.K. Nazeerruddin, A. Kay, I. Rodicio, R. Humphry-Baker, E. Muller, P. Liska, N. Vlachopoulos, M. Grätzel, J. Am. Chem. Soc. 115 (1993) 6382.
[4] M.K. Nazeeruddin, P. Pechy, T. Renouard, S.M. Zakeeruddin, R. Huphry-Baker, P. Comte, P. Liska, L. Cevey, E. Costa, V. Shklover, L. Spiccia, G.B. Deacon, C.A. Bignozzi, M. Grätzel, J. Am. Chem. Soc. 123 (2001) 1613.
[5] T. Shiga, T. Motohiro, Thin Solid Films 516 (2008) 1204.
[6] J.-J. Lagref, Md. K. Nazeeruddin, M. Grätzel, Inorg. Chim. Acta 361 (2008) 735.
[7] L. Giribabu, C.V. Kuma, V.G. Reddy, P.Y. Reddy, C. Srinivasa Rao, S.-R. Jang, J.-Ho Yum, M.K. Nazeeruddin, M. Grätzel, Solar Energy Mater. Solar Cells 91 (2007) 1611.
[8] H. Kusama, M. Kurashige, K. Sayama, M. Yanagida, H. Sugihar, J. Photochem. Photobiol. A: Chem. 189 (2007) 100.
[9] E. Stathatos, P. Lianos, J. Nanosci. Nanotechnol. 7 (2007) 555.
[10] E. Stathatos, P. Lianos, Adv. Mater. 19 (2007) 3338.
[11] S. Ngamsinlapasathian, T. Sreethawong, Y. Suzuki, S. Yoshikawa, Solar Energy Mater. Solar Cells 86 (2005) 269.
[12] S. Ngamsinlapasathian, S. Sakulkhaemaruethai, S. Pavasupree, A. Kitiyanan, T. Sreethawong, Y. Suzuki, S. Yoshikawa, J. Photochem. Photobiol. A: Chem. 164 (2004) 145.
[13] X.B. Chen, S.S. Mao, Chem. Rev. 107 (2007) 2891.
[14] Z.G. Chen, Y.W. Tang, H. Yang, Y.Y. Xia, F.Y. Li, T. Yi, C.H. Huang, J. Power Sources 171 (2002) 990.
[15] I. Zumeta, R. Espinosa, J.A. Ayllon, X. Domenech, R. Rodriguez-Clemente, E. Vigil, Solar Energy Mater. Solar Cells 76 (2003) 15.
[16] (a) E. Stathatos, P. Lianos, U.L. Stangar, B. Orel, P. Judeinstein, Langmuir 16 (2000) 8672;
(b) E. Stathatos, Ionics 11 (2005) 140.
[17] G. Balasubramanian, D.D. Dionysiou, M.T. Suidan, V. Subramanian, I. Baudin, J.-M. Laîné, J. Mater. Sci. 38 (2003) 823.
[18] G. Balasubramanian, D.D. Dionysiou, M.T. Suidan, I. Baudin, J.-M. Laîné, Appl. Catal. B: Environ. 47 (2004) 73.
[19] Y.J. Chen, D.D. Dionysiou, Appl. Catal. B: Environ. 62 (2006) 255.
[20] Y.J. Chen, D.D. Dionysiou, Appl. Catal. A: Gen. 317 (2007) 129.
[21] Y.J. Chen, D.D. Dionysiou, Appl. Catal. B: Environ. 80 (2008) 147.
[22] I. Kei, K. Takashi, Y. Masataka, Y. Shoji, Chem. Commun. 16 (2005) 2131.
[23] G. Balasubramanian, D.D. Dionysiou, M.T. Suidan, in: J.A. Schwarz, C.I. Contescu, K. Putyera (Eds.), Dekker Encyclopedia of Nanoscience and Nanotechnology, 5, Marcel Dekker, Inc., New York, 2004, p. 3917.
[24] H.T. Yang, F.L. Shang, L. Gao, H.T. Han, Appl. Surf. Sci. 253 (2007) 5553.
[25] F. Nishida, J.M. Mckierman, B. Dunn, J.I. Zink, J. Am. Ceram. Soc. 78 (1995) 1640.
[26] L.H. Hu, S.Y. Dai, J. Weng, S.F. Xiao, Y.F. Sui, Y. Huang, S.H. Chen, F.T. Kong, X. Pan, L.Y. Liang, K.J. Wang, J. Phys. Chem. B 111 (2007) 358.
[27] X.C. Wang, J.C. Yu, C.M. Ho, Y.D. Hou, X.Z. Fu, Langmuir 21 (2005) 2552.
[28] J. Wu, S. Hao, Z. Lan, J. Lin, M. Huang, Y. Huang, L. Fang, S. Yin, T. Sato, Adv. Funct. Mater. 17 (2007) 2645.
[29] A.R. Sathiya Priya, A. Subramania, Y.-S. Jung, K.-J. Kim, Langmuir 24 (2008) 9816.
[30] A. Hinsch, S. Behrens, M. Berginc, H. Bönnemann, H. Brandt, A. Drewitz, F. Einsele, D. Faßler, D. Gerhard, H. Gores, R. Haag, T. Herzig, S. Himmler, G. Khelashvili, D. Koch, G. Nazmutdinova, U. Opara-Krasovec, P. Putyra, U. Rau, R. Sastrawan, T. Schauer, C. Schreiner, S. Sensfuss, C. Siegers, K. Skupien, P. Wachter, J. Walter, P. Wasserscheid, U. Würfel, M. Zistler, Prog. Photovolt.: Res. Appl. 16 (2008) 489.
[31] J.M. Kroon, N.J. Bakker, H.J.P. Smit, P. LIska, K.R. Thampi, P. Wang, S.M. Zakeeruddin, M. Grätzel, A. Hinsch, S. Hore, U. Wurfel, R. Sastrawan, J.R. Durrant, E. Palomares, H. Pettersson, T. Gruszecki, J. Walter, K. Skupien, G.E. Tulloch, Prog. Photovolt.: Res. Appl. 15 (2007) 1.